AR-010-468

DSTO

Comparison of CMC and SLF Model Predictions with Experimental Data for Turbulent Hydrogen Jet Flames

Nigel S.A. Smith

DSTO-TR-0631

DEPARTMENT ◆ OF DEFENCE

DEFENCE SCIENCE AND TECHNOLOGY ORGANISATION

COMPARISON OF CMC AND SLF MODEL PREDICTIONS WITH EXPERIMENTAL DATA FOR TURBULENT HYDROGEN JET FLAMES

Nigel S. A. Smith

Airframes and Engines Division
Aeronautical and Maritime Research Laboratory

DSTO–TR–0631

ABSTRACT

Jet diffusion flames have long been the basic model problem for developing and verifying models for turbulent nonpremixed combustion. In this report, a comprehensive jet flame study of two well known models is made as a foundation step for the incorporation of these models into DSTO's ongoing effort to develop a fundamentally-based generic gas turbine combustor predictive capability. Conditional Moment Closure (CMC) and Steady Laminar Flamelet (SLF) model predictions are compared with data measured from the two turbulent hydrogen jet flames studied experimentally by Kent and Bilger, and Barlow and Carter. The comparison highlights the advantages and disadvantages of each model in the context of predicting turbulent nonpremixed flame dynamics in general. The future application of these two models to the turbulent nonpremixed systems associated with gas turbine engine combustors is discussed in the light of the findings presented.

DEPARTMENT OF DEFENCE

DEFENCE SCIENCE AND TECHNOLOGY ORGANISATION

Published by

DSTO Aeronautical and Maritime Research Laboratory
506 Lorimer St,
Fishermens Bend, Victoria, Australia 3207

Telephone: (03) 9626 7000
Facsimile: (03) 9626 7999

AR No. AR-010-468
March 6th 1998

APPROVED FOR PUBLIC RELEASE

Comparison of CMC and SLF model predictions with experimental data for turbulent hydrogen jet flames

EXECUTIVE SUMMARY

Many tasks sponsored by the Australian Defence Force (ADF) have required, and do require, a capability on the part of DSTO to accurately predict the details of turbulent combustion within gas turbine engines. DST Task 95/136 *Gas Turbine Combustor Modelling* represents a pro-active step towards addressing this need through the development of an in-house capability to predict gas turbine combustion.

This report lays the cornerstone for the future development of models to predict turbulent nonpremixed combustion phenomena in gas turbine combustors. It is intended as both an introduction to the combustion modelling problem and a summary of the fundamental capabilities possessed by DSTO. Model development has been proceeding from the point described in this report for some time, largely based on the strength of the analyses presented in this report and elsewhere. The forthcoming reports on current model development will refer to this document as required reading.

The most basic *model problem* for turbulent nonpremixed combustion, such as it occurs in gas turbine engines, is the jet diffusion flame. These experimental-scale flames simply involve passing a gaseous fuel though a nozzle into a coflowing air stream. The turbulent flame of interest sits at the rapidly contorted interface between the fuel and oxidizer streams. Jet flames have the advantage of being easily reproducible, highly accessible for measurement, and possess a flow field which is relatively straightforward to compute. It is for this reason, that most nonpremixed combustion models are trialled against jet flames before being applied to combustion systems of greater complexity and practical interest.

This report describes a comprehensive trial of two sophisticated models for turbulent nonpremixed combustion, namely the Steady Laminar Flamelet (SLF) model and the Conditional Moment Closure (CMC) model. This represents the first time that these two models have been directly compared with one another against comprehensive experimental data sets. The results of this comparison clearly demonstrate the different regimes of applicability of the two models, and their respective accuracies in predicting turbulent flame structure.

A discussion of the implications of the results of these model differences is provided. These lessons are, for the most part, being incorporated into the next generation of the CMC- and SLF-derivative models under development at DSTO; those models include the complicating effects of soot particle dynamics and intense radiant heat transfer to surroundings. The next generation of models is specifically designed for use in complex combustor flows.

THIS PAGE IS INTENTIONALLY BLANK

Author

Nigel S. A. Smith
Airframes and Engines Division

Nigel Smith completed a Bachelor of Engineering with Honours (Mechanical) at the University of Western Australia in 1990. His honours dissertation was a study of flow modification in flat-plate turbulent boundary layers as a result of riblet surface modifications, using laser doppler velocimetry.

Between 1991 and 1994, he studied towards a Ph.D. at the University of Sydney, in the Department of Mechanical Engineering. His research dealt with the development and testing of the Conditional Moment Closure method for predicting turbulent combustion processes. Along the way, he was able to travel and work extensively at the Combustion Research Facility at Sandia National Laboratories in Livermore, California, as well as at Cambridge University and the NATO Advanced Study Institute Workshop in Les Houches, France.

Upon completion of his Ph.D. research and thesis in September of 1994, he took up a position as a postdoctoral fellow at the Center for Turbulence Research, a joint research facility operated by Stanford University and the NASA Ames Research Center. After two years of research into turbulent combustion using direct numerical simulation, he found his way back from Northern California to Melbourne, where he has taken up an RS position in the Airframes and Engines Division.

Nigel Smith's current research objective is to provide DSTO with a credible in-house capability for the prediction of turbulent combustion dynamics in a generic gas turbine combustor setting. The successful implementation of this capability will allow DSTO to better serve the future needs of its customer as they arise, rather than after the fact.

THIS PAGE IS INTENTIONALLY BLANK

Contents

THIS PAGE IS INTENTIONALLY BLANK

1 Introduction

Where combustion takes place in a turbulent fluid flow, the global rate of chemical reactions tend to be greatly increased over that which occurs in a laminar flow. The mixing action facilitated by the turbulent stirring of large scale fluid particles leads to steeper species gradients and thus higher rates of molecular transport to and from reaction zones.

Most combustion systems of engineering interest are configured, in terms of mass flow rates and geometry, to induce turbulent flow and thus capitalise on the high rates of reaction associated with turbulent combustion. An obvious example of such a system is a combustor of a gas turbine engine (henceforth referred to as gas turbine combustor or GTC), where fuel and air react in an essentially nonpremixed mode, with reactions occurring concurrently with molecular mixing at fuel-air interfaces. Another example of tremendous engineering interest is the spark-ignition internal combustion (IC) engine, where fuel and air react in an essentially premixed mode, such that reactions occur behind a highly corrugated thin front which traverses an unburnt mixture.

Currently, nonpremixed combustion modes are employed in GTCs used in aero-propulsion gas turbine units. Nonpremixed configurations avoid much of the difficulty surrounding flame stability which is associated with premixed combustors, particularly when operating over a wide range of conditions. Lean premixed combustors are coming to dominate non-aeronautical gas turbine applications because of their inherently lower pollutant emissions, and because their failure to operate under certain conditions does not have the immediate safety implications that they would have on board an aircraft in flight.

When modelling turbulent nonpremixed combustion, difficulty is encountered in correctly determining mean chemical reaction rates. Unlike in chemically inert turbulent flow, simple Reynolds (or Favre) averaging of the flow field does not provide sufficient information to effect an adequate closure of the resultant averaged scalar equations. The highly non-linear dependence of chemical source terms on local temperature and reactant species concentrations defeats any attempt at a linear first order closure in terms of the averaged local temperature and reactant concentrations. Therefore, a plethora of more sophisticated models have been developed for the prediction of mean chemical reaction rates in turbulent flow. The Steady Laminar Flamelet (SLF) method and Conditional Moment Closure (CMC) methods are two such models which have found application in predicting the behaviour of nonpremixed turbulent combusting flows.

Both of these models are candidates, within the Airframes and Engines Division's (AED) enabling research program on gas turbine combustor modelling, for further application beyond their restricted use in exclusively single (gas) phase combustion. In order for these models to be of practical use in GTC work, they must be integrated with further models for the prediction of multiple-phase combustion phenomena including soot particle and fuel droplet dynamics.

As a first step, however, it is important to evaluate the models in a fundamentally simple single phase combustion environment that is as free from additional submodel inputs as possible. In so doing, the true behaviour of the SLF and CMC models can be determined and model shortcomings and strengths can be identified.

This report is concerned with the evaluation of the SLF and CMC models, against the experimental data of Kent and Bilger[1, 2], and Barlow and Carter[3, 4], for simple hydrogen jet flames issuing into co-flowing air streams. Characteristic failings in the predictive capability of each model are highlighted against the observed experimental data, and speculations are made as to what impact these failings will have on future model use within the context of GTC research.

2 Modelling Methods

In advance of discussing the combustion models themselves, it is appropriate, in this forum, to provide additional background information which will aid in understanding the results and discussion which will follow this section.

The prediction of turbulent nonpremixed combustion can in most cases be reduced to a problem which is largely governed by the rate of mixing of fuel and oxidizer. This is probably why there has been substantial progress in nonpremixed model development compared to the development in predicting turbulent premixed combustion, where the interaction between flame and flowfield is more intimate.

The local instantaneous equation for the conservation of the mass fraction (Y_α) of a chemical species (α) can be written as,

$$\frac{\partial}{\partial t}(\rho Y_\alpha) + \frac{\partial}{\partial x_i}(\rho u_i Y_\alpha) - \frac{\partial}{\partial x_j}(\rho \mathcal{D}_\alpha \frac{\partial Y_\alpha}{\partial x_j}) = \rho \dot{w}_\alpha \tag{1}$$

where ρ is the fluid density, u_i is the i-th component of fluid velocity, $\mathcal{D}_\alpha$ is the molecular diffusivity (Fickian diffusion approximation) of the species α, and $\dot{w}_\alpha$ is the net chemical production rate of α. Note that the convention is adopted throughout this report that summation over terms bearing roman subscripts is implied, while terms bearing greek subscripts are not subject to summation unless explicitly stated.

A useful measure of the degree of mixing between fuel and oxidizer masses is provided by the chemically conserved scalar known as mixture fraction (ξ). Mixture fraction is a scalar which is derived from an appropriate linear combination of chemical scalars,

$$\xi \equiv \sum_{\alpha=1}^{N} a_\alpha Y_\alpha \tag{2}$$

such that the net chemical production of the scalar is identically zero,

$$\sum_{\alpha=1}^{N} a_\alpha \dot{w}_\alpha = 0 \ , \tag{3}$$

and is normalised so that (by convention) it has a value of unity in fluid that originated wholly from the fuel stream, and zero in fluid that originated in the oxidizer stream.

It is necessary to refer to fuel and oxidizer 'origins' since while fuel and oxidizer may be chemically consumed in an isolated sample, the mixture fraction will remain unchanged. Thus the resultant mixture of products and remnant reactants will constitute the same

value of mixture fraction as the original unreacted sample. Only the introduction of further mass (through mixing) to change the atomic population of the sample will have any bearing on mixture fraction. It is this invariance under reaction which makes mixture fraction such a useful *coordinate* in which to examine nonpremixed combustion.

The conservation equation for mixture fraction is derived from the same linear combination of species equations as was used to define the scalar,

$$\frac{\partial}{\partial t}(\rho\xi) + \frac{\partial}{\partial x_i}(\rho u_i \xi) - \frac{\partial}{\partial x_j}(\rho \mathcal{D}_\xi \frac{\partial \xi}{\partial x_j}) = 0 \tag{4}$$

where $\mathcal{D}_\xi$ is the weighted aggregate of the individual species molecular diffusivities.

It is always possible to define a mixture fraction, irrespective of the chemical scheme in question, since by their very nature chemical reactions always conserve atomic species. Where the molecular diffusivities of all species are uniform, mixture fraction is a unique scalar that will have the same value at a given composition independently of the details of its definition. Where the diffusivities are significantly disparate, the local value of mixture fraction is definition dependent and the uniqueness of the scalar is lost [5]. In practice, it is usually assumed that all species diffusivities are uniform so as to simplify the analysis and remove the ambiguity associated with having many different mixture fractions.

2.1 Fast Chemistry Assumption

Some of the earliest models for nonpremixed combustion made use of a parameterisation of chemical state as a function of mixture fraction[6]. The basis for these 'fast chemistry' methods lies in the assumption that the chemical reactions associated with combustion are much faster than the mixing processes that bring reactant and oxidizer together. In the limit of infinitely fast chemical reaction rates, the width of the flame zone between fuel and oxidizer shrinks to zero, centred on a surface corresponding to the stoichiometric mixture fraction.

In this case the requirement to solve for chemical source terms is eliminated since the problem is reduced to one of inert mixing between three mixture fraction states, namely pure fuel, pure oxidizer and a stoichiometric mixture of chemical equilibrium products.

Under the fast chemistry assumption, the mean temperature and species concentration fields are wholly described by the equations for the Favre mean $\langle\xi\rangle$,

$$\bar{\rho}\frac{\partial\langle\xi\rangle}{\partial t} + \bar{\rho}\langle u_i\rangle\frac{\partial\langle\xi\rangle}{\partial x_i} - \frac{\partial}{\partial x_j}(\bar{\rho}\mathcal{D}_\xi\frac{\partial\langle\xi\rangle}{\partial x_j}) = -\frac{\partial}{\partial x_i}(\langle u_i'\xi'\rangle) \tag{5}$$

and variance $\langle\xi'^2\rangle$ of mixture fraction,

$$\bar{\rho}\frac{\partial\langle\xi'^2\rangle}{\partial t} + \bar{\rho}\langle u_i\rangle\frac{\partial\langle\xi'^2\rangle}{\partial x_i} - \frac{\partial}{\partial x_j}(\bar{\rho}\mathcal{D}_\xi\frac{\partial\langle\xi'^2\rangle}{\partial x_j}) = -\frac{\partial}{\partial x_i}(\langle u_i'\xi'^2\rangle) - 2\bar{\rho}\langle u_i'\xi'\rangle\frac{\partial\langle\xi\rangle}{\partial x_i} - 2\bar{\rho}\mathcal{D}_\xi\langle(\frac{\partial\xi}{\partial x_j})^2\rangle \tag{6}$$

and the pre-computed chemical equilibrium species/temperature states as functions of mixture fraction.

This methodology has the distinct advantage of being no more expensive, in terms of computational resources, than solving for a passive contaminant in the flow. Naturally, however, its principle disadvantage lies in the fact that all chemical reaction rates are not all much faster than mixing rates in all cases.

Problems associated with the temporal coupling between timescales for chemical reactions and mixing processes, such as local extinction and pollutant formation, have provided a strong motivation for the development more sophisticated models. Two of these models are discussed in the remainder of this report, however the reader is reminded that many other equally versatile models exist[7, 8, 9, 10].

2.2 Steady Laminar Flamelet Model

The Steady Laminar Flamelet (SLF) model, first employed in turbulent nonpremixed combustion by Peters[11], retains the concept of parameterizing the nonpremixed system in terms of mixture fraction. However, the SLF model incorporates a further parameter which accounts, to some degree, for the finite rates of chemical reaction in comparison to the local rate of mixing.

The basic assumption of the SLF model is that the structure of flame zones in turbulent flow is identical to that which would occur in a steady one-dimensional laminar diffusion flame under the same local rate of flow field strain. Under these conditions, the conservation of any chemical species can be written as,

$$\frac{\partial}{\partial x}(\rho(u + V_\alpha)Y_\alpha) = \rho\dot{w}_\alpha \tag{7}$$

where V_α is the local diffusion velocity, and x is the direction perpendicular to the flame isopleths.

In practice, a large number of steady one-dimensional laminar flamelet calculations are performed for a counterflow diffusion flame configuration at different strain rates imposed by the counterflowing velocities. The thermochemical composition is taken and recorded in a flamelet *library* at regular mixture fraction stations throughout the flames for each strain rate case. Later, when used in predicting turbulent combustion, the flamelet library data is used to specify local flame conditions given the local mean rate of strain (or scalar dissipation rate), and mixture fraction. Mean flame conditions are determined through convolution of appropriate library data with an assumed-form mixture fraction probability density function (PDF), which is parameterized in terms of the local mixture fraction mean and variance.

Implicit in the SLF model, is the underlying assumption that the *flame zones* are thin compared to the smallest scales of turbulent motion which convectively modify the composition field around the flame.

The notion of a *flame zone* is problematic, in that it means different things to different participating species; principle zones of reaction (flame zones) will be thin for rapidly reacting species, while broad for slowly reacting species[12, 13]. For example, species such as nitric oxide (NO) which have a low rate of formation, effectively have a principal reaction zone which is not confined to thin laminae and can span the global volume of

reacting fluid. Kinetically-limited species such as NO are usually considered to be outside the domain of SLF models and are typically treated separately.

Species with high molecular diffusivities (such as the monatomic hydrogen radical, H) are less likely to the remain in a locally one-dimensional structure when in the presence of substantial flow-induced flame curvature. Thus it is likely that under strong turbulent mixing, the diffusional transport of many key species to and from the reaction zone will not be locally one-dimensional, and thus not well represented by steady laminar flamelet data. Stårner *et al.*[14] provide experimental evidence of substantial departure from flamelet behaviour, due to strong local curvature and associated influences, in various hydrocarbon flames.

The application of steady laminar flamelet data to turbulent flow involves the assumption that the speed of local mixing transients are slow compared to the reaction times of the local thermo-chemistry[13]. Some effort has been made to investigate the significance of unsteadiness in flames of interest[15, 16, 17, 18], and even to utilize a generalised unsteady laminar flamelet method[19].

Despite all of the misgivings outlined above, the SLF model remains a very versatile and computationally attractive method. As with the fast chemistry model, the actual peruse computational overhead involved in using the model is no more than that of solving for the transport of a passive scalar.

Peters[20, 21] provides an excellent review and discussion of SLF model application in the prediction of turbulent nonpremixed combustion.

2.3 Conditional Moment Closure Method

The Conditional Moment Closure (CMC) method, proposed independently by Klimenko [22] and Bilger[23], does not involve an *a priori* parameterisation of nonpremixed flames. This approach allows for flame structures which are not necessarily thin compared to the smallest scales associated with species mixing. The CMC method allows for species development on timescales much greater than the local mixing timescales. This flexibility comes at a cost however; the computational expense associated with CMC calculations is typically much greater than the cost of solving for a passive contaminant[24].

The CMC method involves solving for the mean species mass fractions which result from conditionally averaging an ensemble of instantaneous local realisations of the turbulent flow in question. The conditional mean quantities are determined by discriminating between contributing samples on the basis of their associated value of mixture fraction. For a given conditioning value (η) of mixture fraction (ξ), only those samples simultaneously meeting the conditional criteria ($\xi(\underline{x},t) = \eta$) are allowed to contribute to the mean. Thus instead of traditional *un*conditional averaging, where averaging over an ensemble of points in time and space would only produce a single value, the conditional averaging process produces a profile of mean values,

$$Q_\alpha(\underline{x},t,\eta) \equiv \langle Y_\alpha(\underline{x},t) \mid \eta \rangle, \tag{8}$$

as a function the conditioning variable abscissa (η).

Conditional averaging of the corresponding instantaneous species mass fraction equations (eq 1) yields,

$$\langle \rho \mid \eta \rangle \frac{\partial Q_\alpha}{\partial t} + \langle \rho u_i \mid \eta \rangle \frac{\partial Q_\alpha}{\partial x_i} = \frac{1}{2} \langle \rho \chi \mid \eta \rangle \frac{\partial^2 Q_\alpha}{\partial \eta^2} + \langle \rho \dot{w}_\alpha \mid \eta \rangle, \tag{9}$$

where χ is the instantaneous scalar dissipation rate defined by,

$$\chi \equiv 2\mathcal{D}_\xi (\frac{\partial \xi}{\partial x_j})^2. \tag{10}$$

Equation (9) neglects the contributions of small deviations from the conditional means of species mass fraction and velocity, as well as terms associated with the molecular transport of conditional means species mass fractions in physical space[22]. The latter omission is justified in flows at high Reynolds numbers, with the bulk of species transport being carried by turbulent motion to all but the smallest scales.

In order to conserve mass in the overall system of equations, it is essential that the conditional mean scalar dissipation rate be determined from the companion equation for the probability density function (PDF) of mixture fraction (P_η),

$$\frac{\partial}{\partial t}(\langle \rho \mid \eta \rangle P_\eta) + \frac{\partial}{\partial x_i}(\langle \rho u_i \mid \eta \rangle P_\eta) = -\frac{1}{2} \frac{\partial^2}{\partial \eta^2}(\langle \rho \chi \mid \eta \rangle P_\eta). \tag{11}$$

In practice, the CMC equations (9) are solved in concert with the unconditional moment equations for mixture fraction (eqs 5 & 6), and the evolution of the mixture fraction PDF is then assumed to correspond with the changes in an assumed-form PDF. The conditional mean scalar dissipation rate ($\langle \rho \chi \mid \eta \rangle$) is then determined through the double integration of the left hand side of the PDF equation (11), followed by division by the PDF itself.

Closure of the conditional mean chemical production term ($\langle \rho \dot{w}_\alpha \mid \eta \rangle$) can be effected using a first order approximation involving only the conditional mean reactant species and temperature upon which each reaction depends,

$$\langle \dot{w}_\alpha(Y_1, Y_2, \ldots, Y_N, T) \mid \eta \rangle \approx \dot{w}_\alpha(Q_1, Q_2, \ldots, Q_N, \langle T \mid \eta \rangle). \tag{12}$$

The chemical closure is only accurate whilst the level of instantaneous deviations from the conditional mean reactive scalar values are *sufficiently* small. The determination of what is sufficiently small varies according to the chemical reaction being approximated. Reactions with particularly high activation temperatures or other temperature dependencies, tend to be proportionally more sensitive to the influence of deviations from conditional means[25], and so can only tolerate very low levels of fluctuations.

Significantly, first order chemical closure is particularly dubious in flames which are nearing extinction conditions[12]. It has been observed [26]-[30] that flames close to extinction exhibit high levels of deviation from conditional means, such that closure of even the most insensitive reaction is problematic.

As written and implemented, the CMC species equations (9) make no allowance for the effects of widely disparate molecular diffusivities. In cases where turbulent mixing action

is the overwhelming mechanism responsible for species mixing, the influence of differential species diffusion can reasonably be supposed to be small. Regions where this is most likely to break down are those where the flame is particularly thin compared to the mixing length scales, such that molecular diffusion is predominant in the large gradients between fuel and oxidizer.

Differential diffusion in nonpremixed combustion has been observed to significantly elevate the level of deviations from conditional means [31], which then serves to further hamper the first order chemical closure (eq 12). Treatments for differential diffusion within the CMC framework have been proposed for inert mixing[32], but the application of this treatment to reactive systems is still untested.

The CMC method has been successfully applied on a number of occasions in the prediction of jet flame structure[24, 33, 34], particularly in relation to the prediction of NO_x formation. The CMC method avoids many of the shortcomings of the SLF method, albeit at significant computational cost, and so is a likely candidate as an advanced post-processing tool for the refinement of SLF model predictions.

2.3.1 Radiant loss submodel

Unlike the SLF model, the CMC model is readily amenable to the incorporation of radiant heat loss into the system of equations. In the case of jet flames, it is assumed that the loss of heat from the flame through radiation occurs in the optically thin regime.

In this regime, photons of radiated energy emanate from points of origin within the flame and are not reabsorbed by any other part of the flame as they make their way out of the computational domain.

The instantaneous heat loss per unit volume of emitting gas ($\dot{s}$) is given by,

$$\dot{s} = 4\sigma T^4 \sum_{\alpha=1}^{N} \kappa_\alpha(T) p_\alpha \tag{13}$$

where $\kappa_\alpha(T)$ is the Planck mean absorption coeficient for emitting species α, p_α is the partial pressure of the species α, T is the local temperature, and σ is the Stefan-Boltzmann constant.

The conditional mean radiant heat loss rate ($\langle \dot{s} \mid \eta \rangle$) appears as a source term on the right hand side of a CMC equation, for standardised enthalpy instead of species mass fraction. Closure of this source term is carried out as a first order approximation as in equation (12).

2.3.2 Parabolic flow configuration

The CMC equations can be significantly simplified in terms of dimensionality when applied to cases of steady parabolic flow (eg. jets, mixing layers, far-field wakes etc.). In these instances, the variation in cross-stream *conditional* mean quantities was predicted[5, 35], and was found[4], to be negligible at all axial locations but those very close to the upstream mixing interface (eg. nozzle in the case of a jet).

The steady cross-stream averaged CMC equations[24, 35] are simply derived from equation (9) and involve the use of cross-stream averaged determinations of conditional mean scalar dissipation rate ($\langle \chi \mid \eta \rangle$), and conditional mean axial velocity ($\langle u \mid \eta \rangle$) [24].

As with all CMC model computations, conventional (unconditional) mean values of species mass fractions, temperature, enthalpy, and reaction rates can be obtained at any time through convolution of the conditional statistics with the local mixture fraction PDF,

$$\langle Y_\alpha(x,r) \rangle = \int_{\eta=0}^{\eta=1} Q_\alpha(x,\eta) P_\eta(x,r,\eta) d\eta. \tag{14}$$

Currently, a beta function assumed-form PDF is being employed for convolution of conditional mean data, and computation of conditional mean scalar dissipation rate from equation (11).

2.4 Model implementation

The SLF and CMC models were used in conjunction with a computational fluid dynamic (CFD) software package known as TASCflow3D, which is a proprietary product of AEA Technology - Advanced Scientific Computing. The SLF model is an existing optional feature of TASCflow3D, while the CMC model is used in a postprocessing role with its parent code (AFTJET-II) accepting TASCflow3D output as input.

The well known $k - \epsilon$ turbulence model described by Launder and Spalding [36] was used in the TASCflow3D code with standard model coeficients. The turbulent Prandtl number was set to 0.9 while all species Lewis numbers (including mixture fraction) were set to unity.

The chemical mechanism used in the CMC calculations and in the generation of the SLF flamelet library is provided in Table 1 and constitutes the non-carbon steps of the wet-CO starting mechanism of Rogg and Williams[37], as well as selected steps of the NO_x thermal pathway described by Miller and Bowman[38].

No.	Reaction Description	A	α	E_a
1f.	$O_2 + H \rightarrow OH + O$	2.00E14	0.00	16800.
1b.	$OH + O \rightarrow H + O_2$	1.57E13	0.00	841.3
2f.	$H_2 + O \rightarrow OH + H$	5.06E04	2.67	6286.
2b.	$H + OH \rightarrow O + H_2$	2.22E04	2.67	4371.
3f.	$H_2 + OH \rightarrow H_2O + H$	1.00E08	1.60	3298.
3b.	$H_2O + H \rightarrow H_2 + OH$	4.31E08	1.60	18274.
4f.	$O + H_2O \rightarrow OH + OH$	1.47E10	1.14	16991.
4b.	$OH + OH \rightarrow H_2O + O$	1.59E09	1.14	100.4
5.	$H + O_2 + M \rightarrow HO_2 + M$	2.30E18	-0.80	0.00
6.	$H + HO_2 \rightarrow OH + OH$	1.50E14	0.00	1004.
7.	$H + HO_2 \rightarrow H_2 + O_2$	2.50E13	0.00	693.1
8.	$H + HO_2 \rightarrow H_2O + O$	3.00E13	0.00	1721.
9.	$OH + HO_2 \rightarrow H_2O + O_2$	6.00E13	0.00	0.00
10.	$O + HO_2 \rightarrow OH + O_2$	1.80E13	0.00	-406.3
11.	$HO_2 + HO_2 \rightarrow H_2O_2 + O_2$	2.00E12	0.00	0.00
12f.	$HO_2 + H_2O \rightarrow H_2O_2 + OH$	2.86E13	0.00	32790.
12b.	$H_2O_2 + OH \rightarrow HO_2 + H_2O$	1.00E13	0.00	1800.
13f.	$H_2O_2 + M \rightarrow OH + OH + M$	1.30E17	0.00	45500.
13b.	$OH + OH + M \rightarrow H_2O_2 + M$	9.86E14	0.00	-5070.
14.	$H_2O_2 + H \rightarrow HO_2 + H_2$	1.60E14	0.00	3800.0
15.	$OH + H + M \rightarrow H_2O + M$	2.20E22	-2.00	0.00
16.	$H + H + M \rightarrow H_2 + M$	1.80E18	-1.00	0.00
17.	$O + O + M \rightarrow O_2 + M$	1.89E15	0.00	-1788.0
18.	$O + N_2 \rightarrow NO + N$	1.40E14	0.00	75800.
19.	$N + O_2 \rightarrow NO + O$	6.40E09	1.00	6280.
20.	$OH + N \rightarrow NO + H$	4.00E13	0.00	0.00
21.	$NO + HO_2 \rightarrow NO_2 + OH$	2.11E12	0.00	-480.
22.	$NO_2 + H \rightarrow NO + OH$	3.50E14	0.00	1500.

Table 1: Chemical Mechanism employed for H_2-air combustion, units of cal, K, mol, m, s

Flame Designation	KB	BC
References	[1, 2]	[3, 4]
Nozzle Diameter (D) [mm]	7.62	3.75
Bulk Jet Velocity (U_j) [m/s]	146	300
Coflow Air Velocity (U_c) [m/s]	15.0	1.00
Cold Jet Reynolds Number	7,000	10,000
Convective Timescale (D/U_c) [s]	5.2e-5	1.2e-5
Stoichiometric Flamelength (L_{st}/D)	$\sim$ 135	$\sim$ 135
Test section diameter [mm]	305	n/a
Diagnostic techniques	physical	optical

Table 2: Observed H_2 flame conditions and characteristics

3 Results

The salient features of the turbulent hydrogen jet flames being studied can be found in Table 2. The flame of Kent and Bilger[1] (henceforth designated KB), was surrounded by the walls of a vertical wind tunnel test section and burnt at atmospheric pressure. The ratio of the tunnel diameter to the nozzle inner diameter was approximately forty (40), and care was taken to ensure that the axial pressure gradient through the test section was minimized. The recorded data taken from flame KB included pitot tube measurements of velocity statistics, thermocouple measurements of mean temperatures, and gas sample probe measurements of mean compositions. When the data was published in 1974, it was widely accepted as a definitive description of a turbulent hydrogen jet flame.

The more recent data of Barlow and Carter[3] taken from a jet flame (designated here as BC) represent a closer look at this fundamental combustion paradigm. Instantaneous point measurements of major species concentrations, temperature, and concentrations of nitric oxide (NO) and hydroxyl radical (OH) were made using a combination of Rayleigh and Raman spectroscopy and laser induced fluorescence (LIF). The ability to examine the actual instantaneous levels of chemical species in flame BC, instead of mean concentrations, allows a far superior analysis of the flame dynamics and provides a superior gauge of model behaviour.

Flames KB and BC are comparable in many respects; they have similar Reynolds numbers, fuel type, and stoichimetric flamelengths. The principal difference between the two flames can be found in their convective timescales. These values can be used as a guide to the actual period of time parcels of nozzle fluid remain within the stoichiometric envelope. Flames with longer convective timescales, all else being equal, tend to lose greater amounts of heat through radiation and emit greater amounts of kinetically-limited species (eg. soot/smoke, oxides of nitrogen).

In computing the mixing field enveloping flames KB and BC with a $k - \epsilon$ turbulence model, it was found that there were qualitative differences between predictions and observations of the development of the mixture fraction field. The nature of these differences can be seen from Fig. 1 where the decay in centreline mean mixture fraction with axial distance from the nozzle in flame BC is compared for the various data sources. Note

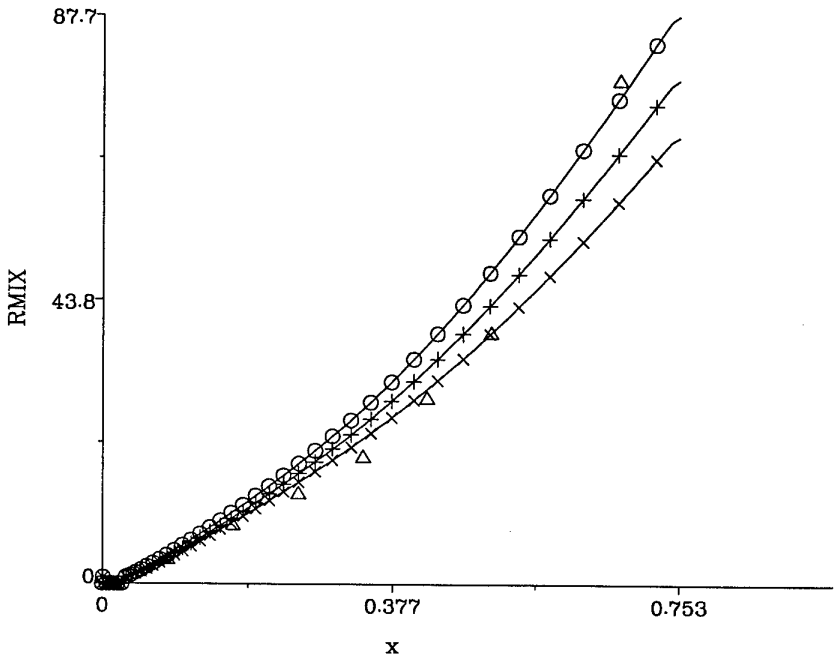

Figure 1: Centreline reciprocal mean mixture fraction for flame BC as a function of axial distance from nozzle (m). Note nozzle diameter is 3.75 mm. Symbol key: (cross) Pr_t = 0.9, (plus) Pr_t = 0.8, (circle) Pr_t = 0.7, (delta) experimental measurement.

that the reciprocal of mean mixture fraction is plotted in the figure to facilitate a clear comparison of downstream differences between the profiles.

Three different values of turbulent Prandtl number were used in generating predictions, in an effort to best match the experimentally observed profile. It is clear that the experimental decay in centreline mixture fraction drops more gently than all of the predicted curves out to about 100 diameters from the nozzle, before dropping more sharply out to the 180 diameter final station. Note that the 0.753 position on Fig. 1 corresponds to a distance 200 diameters from the nozzle.

Calculations with a turbulent Prandtl number of $Pr_t = 0.9$ were used in subsequent analyses since these calculations provided best agreement in terms of predicting the stoichiometric flamelength (see Table 2) correctly, albeit at the expense of accuracy further downstream.

Non-standard variants of the $k - \epsilon$ model are claimed to provide superior mixing predictions in a jet flow[2]. Predictions with more sophisticated second order turbulence models[34] have not shown the same discrepancies as was seen in Fig. 1, however these models are not currently available in a useable form at DSTO.

3.1 Unconditional mean data

The basic nature of the predicted unconditional mean form of the jet flames can be seen in Fig. 2. In the figure, greyscale intensity maps of unconditional mean temperature and hydroxyl mole fraction (OH) are presented for the entire axisymmetric computational domain. The maps specifically correspond to CMC predictions for flame KB, but are qualitatively similar to all of the predictions and observations for the flames studied here.

Pure H_2 fuel enters the domain through the nozzle at the bottom of each map in a small region centred about $y = 0$. Air is entrained from outside this zone and mixes with the fuel in the jet such that a stoichiometric contour forms where the fuel and oxidizer are in the correct proportions so that neither is in excess.

Chemical activity is essentially confined to the vicinity of this contour; high energy radical species such as OH are produced and consumed nearby. The approximate location of the stoichiometric contour can be inferred from the thin zones of high OH mole fraction indicated in Fig. 2. Note that the reaction zone is particularly narrow in the upstream portion of the flame, where mean mixture fraction gradients are high. Further downstream, the band of high OH is broadened as the mean mixture fraction gradients decrease and the relative importance of turbulent fluctuations increase. The reaction zones are distributed in these regions, rather than being confined to thin laminae. Beyond the stoichiometric flamelength, where the inner contour of OH map closes, residual hydroxyl radicals flow downstream whilst being rapidly consumed in cooler leaner parts of the flame.

High temperature zones are in evidence about the stoichiometric surface. The local mean temperatures increase along the length of the contour out from the nozzle exit plane, as the strength of turbulent mixing processes decays and the chemical system is allowed to move closer to a fast-chemistry equilibrium state. The peak mean temperature occurs slightly short of the location where the stoichiometric contour crosses the centreline. Beyond this point, the release of heat through the evolution of exothermic products gradually subsides. The behaviour of the flame is thereafter like that of a heated jet, losing heat through a combination of radiant losses and the entrainment of cooler surrounding fluid.

3.1.1 Flame of Kent and Bilger (KB)

The quantitative trend in centreline unconditional mean temperature ($\langle T \rangle_c$) with axial displacement from the nozzle (x) of flame KB, can be gauged from Fig. 3. The measured evolution of mean temperature is compared with that predicted using the SLF and CMC methods, as well as the curve resulting from the application of a fast chemistry approximation. The reader is reminded that the nozzle diameter corresponding to flame KB was 7.62 mm, and so the axial range plotted in Fig. 3 covers the first two hundred diameters of flow.

It is evident that there is good agreement between all predictive methods and the observed profiles out to about forty (40) diameters. Thereafter, the SLF model is in good agreement with the measured profile out to around eighty (80) diameters. The SLF predictions and measured profile diverge from this point, with the CMC model then providing better agreement with the measured behaviour. The peak centreline temperature predicted by the CMC model agrees to within five (5) degrees Kelvin of the measured

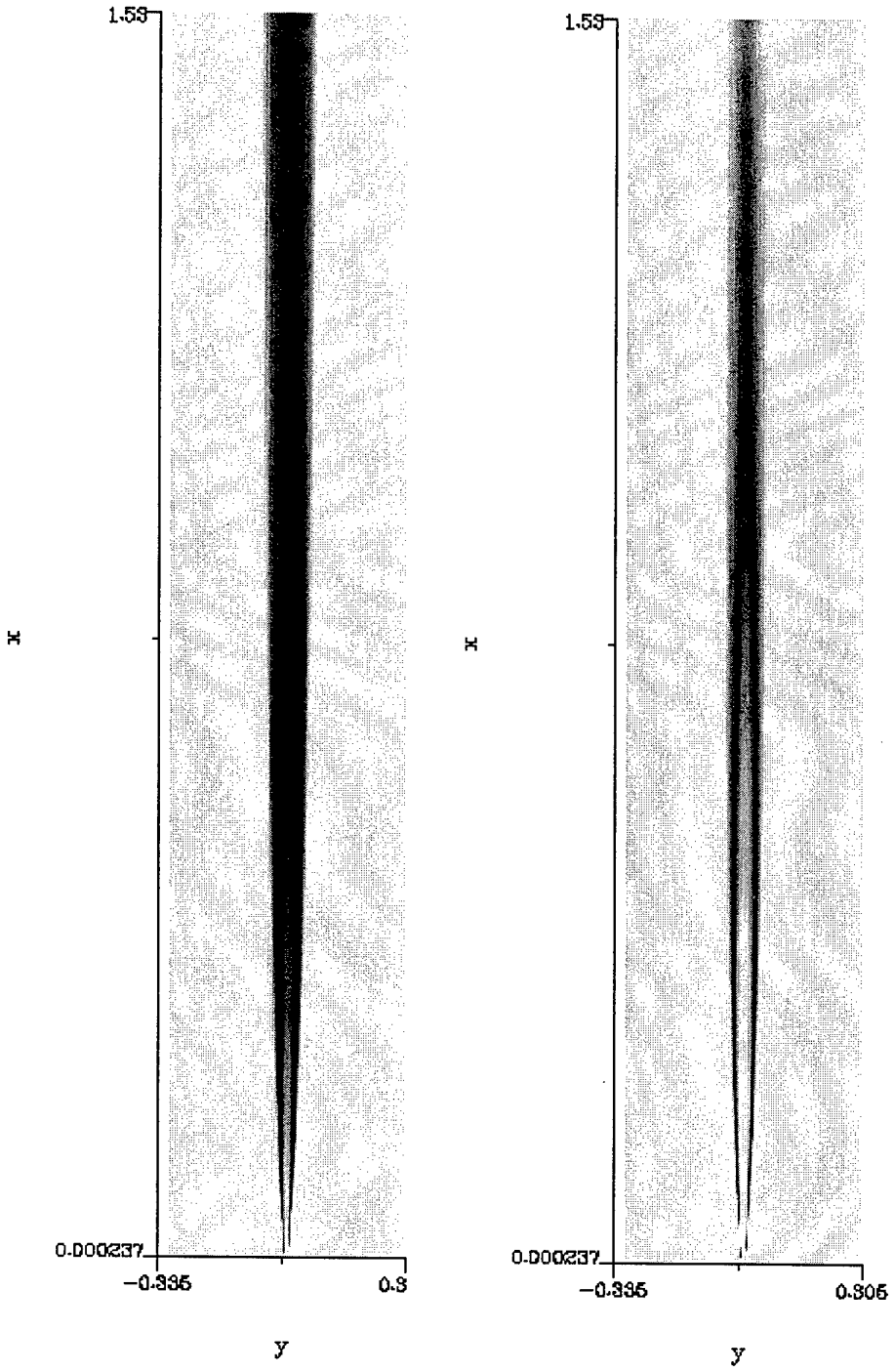

Figure 2: Predicted mean temperature (left) and OH mole fraction (right) distributions. (Temperature : white 300 K - black 2150 K, OH mole fraction : white 0 - black 3.7e-3)

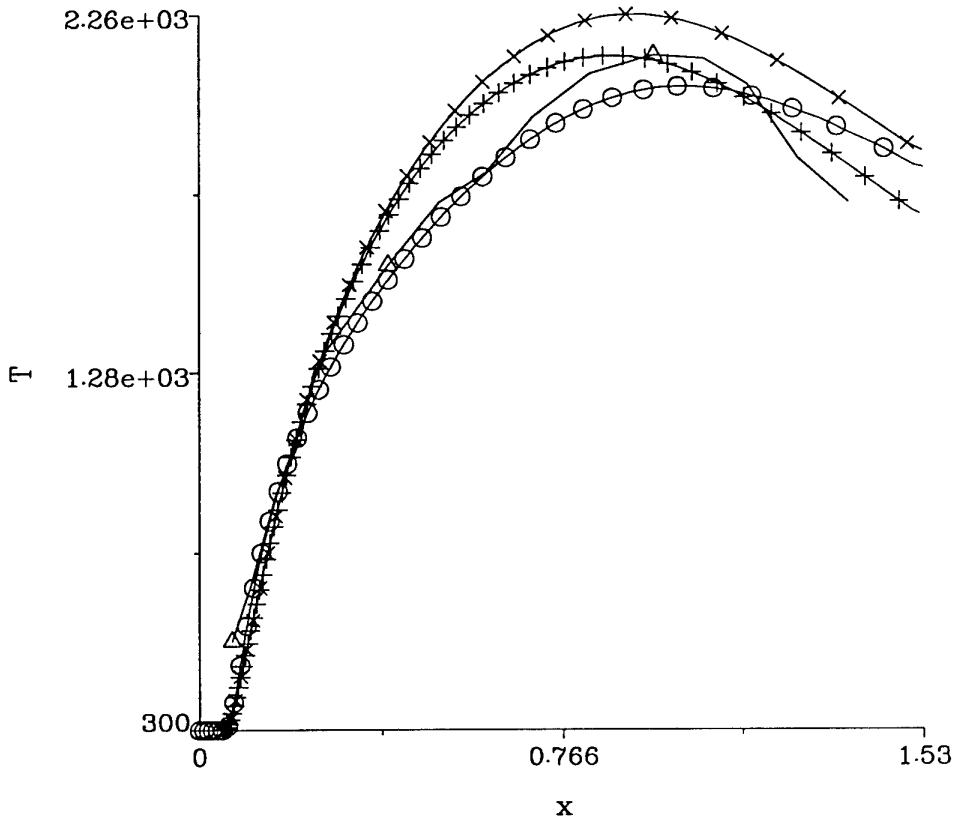

Figure 3: Centreline mean temperature (K) for flame KB as a function of axial distance from nozzle (m). Note nozzle diameter is 7.62 mm. Symbol key: (cross) fast chemistry, (plus) CMC, (circle) SLF, (delta) experimental measurement.

profile, but its axial location is about eight (8) diameters closer to the nozzle than what was observed experimentally. The SLF model predicts a peak centreline mean temperature which is approximately one hundred and twenty (120) degrees Kelvin cooler than the measured value, but the location of the peak is closely predicted.

Downstream of the predicted peaks, the temperature profile predicted by SLF model nears the profile corresponding to an adiabatic fast chemistry approximation. The CMC model, however, deviates progressively further from the equilibrium profile with axial length, under the influence of radiant losses and in keeping with the measured profile. Towards the end of the flame, the CMC predicted and measured profiles have a similar slope in the axial direction.

Predicted and measured radial distributions of mean temperature in flame KB are plotted for axial locations of $x/D = 80$, 120, & 160 in Fig. 4. The maximum radial extent

of the abcissa in each plot corresponds to approximately ten diameters, or twenty times the inner radius of the nozzle. Both models reflect the measured behaviour quite closely at all of the axial measurement stations. They capture the observed shift towards the centreline of the radial location of greatest mean temperature. This movement roughly follows the location of the mean stoichiometric contour; it is evident that the contour crosses the centreline between the first two radial-traverse stations.

It is apparent that the CMC model predictions for temperature are significantly greater than the corresponding SLF model predictions at the two upstream locations. A cross-over in model predictions is observed at the location furthest downstream, where radiant losses have resulted in substantial cooling in the case of the CMC model. Notice that the cooler temperatures associated with radial zones removed from the centreline, at $x/D = 160$, do not exhibit the same degree of depression as those on the centreline. This is as you would expect given the high power dependence of radiant losses upon local temperature, so that the relative magnitude of losses in cooler zones is much lower.

3.1.2 Flame of Barlow and Carter (BC)

The nature of flame BC is such that it is less affected by radiative heat losses than the longer residence time flame, KB. The shorter length of time that fluid is within the high temperature zones of the flame reduces the the amount of heat which is emitted as radiation relative to the amount which is chemically evolved.

This fact is apparent after careful comparison of the centreline mean temperature development in flame BC (Fig. 5), and the corresponding trend in flame KB (Fig. 3). The separation between the CMC and adiabatic fast-chemistry predicted temperature curves is significantly greater (of order $\sim$ 200 K) in the downstream portion of flame KB than in flame BC (of order $\sim$ 20 K). Unlike the behaviour evident from Fig. 3, the SLF-predicted temperature curve for flame BC agrees closely with both the CMC and adiabatic fast-chemistry profiles in the tail of the flame.

The CMC and SLF models demonstrate the same behaviour as was observed in flame KB (see Fig. 3), in regard to the magnitude and location of the centreline peak mean temperature. All of the modelling methods overpredict the centreline temperature at the end of the flame by hundreds of degrees Kelvin. This consistent error can be explained in terms of the particularly poor agreement between the measured and predicted mixture fraction fields in this vicinity (see Fig. 1). The tendency of the turbulence model to greatly overestimate the level of centreline mean mixture fraction from $x/D \sim 140$ onwards, has the effect of limiting the rate at which the hot flame gases are diluted with cold air.

The radial variation of predicted and measured temperature for flame BC is plotted in Fig. 6 at nondimensional axial stations of $x/D = 45, 90, 135$ & 180. It is again apparent that the predicted profiles have resulted from an underpredicted mixing rate of jet fluid with coflowing fluid. At the downstream stations, it is clear that the measured temperature profiles are increasingly broad with axial length, over and above that exhibited by the predictions. This tendency is further borne out by an analysis of the radial distributions of mean mixture fraction (not plotted).

At all stations barring the last, it appears that the high temperature sections of the measured profiles are best predicted by the CMC model.

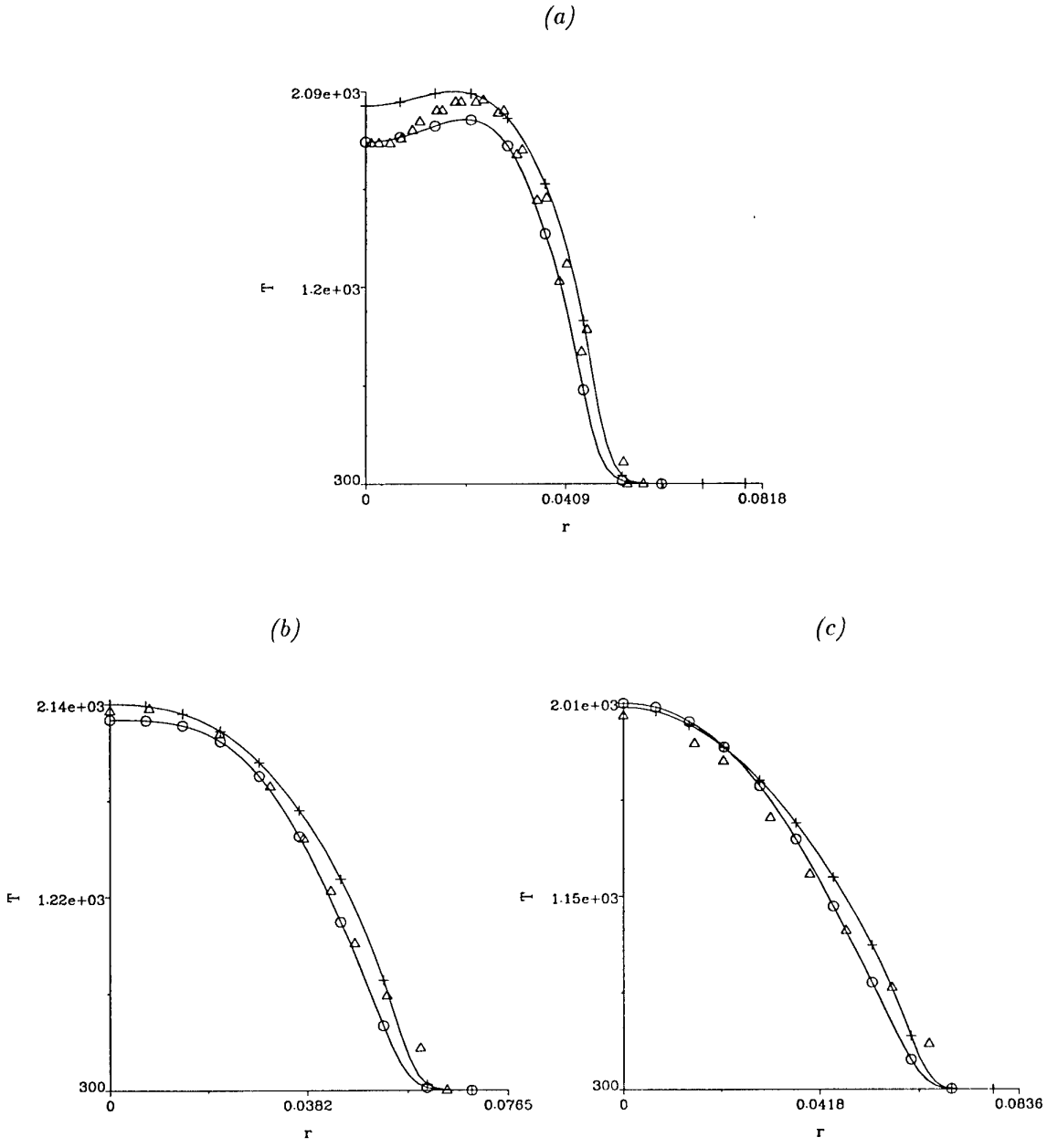

Figure 4: Radial variation in mean temperature at x/D = 80 (a), 120 (b), 160 (c) in flame KB. Note nozzle diameter is 7.62 mm. Symbol key: (plus) CMC, (circle) SLF, (delta) experimental measurement.

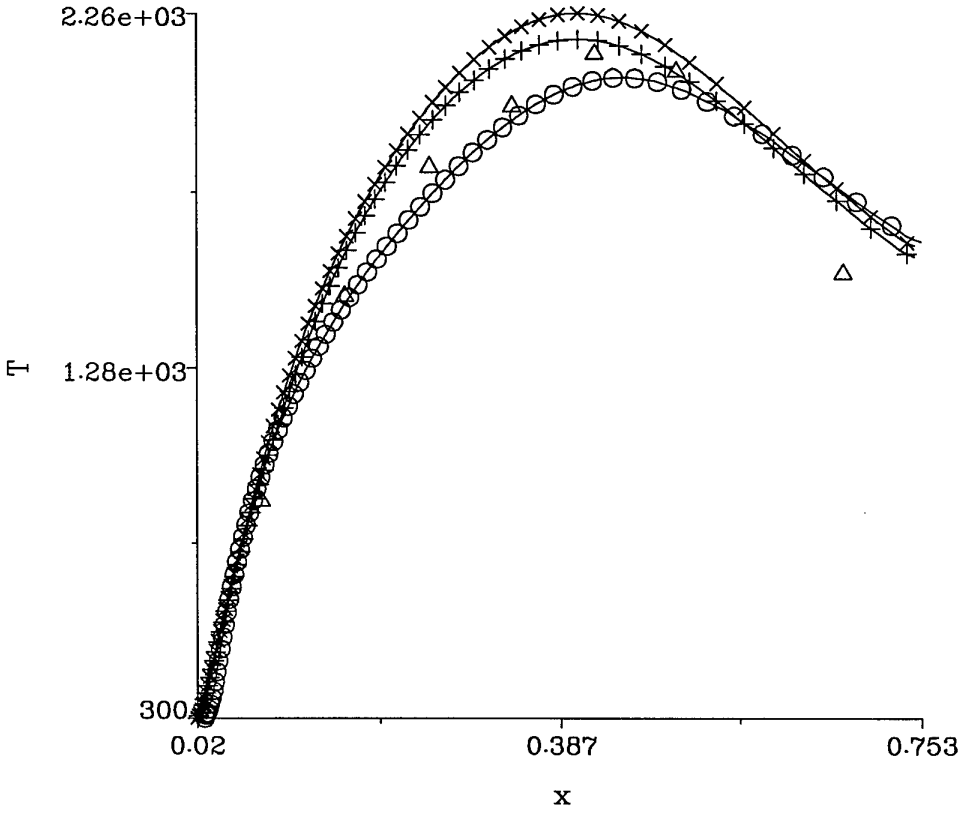

Figure 5: Centreline mean temperature (K) for flame BC as a function of axial distance from nozzle (m). Note nozzle diameter is 3.75 mm. Symbol key: (cross) fast chemistry, (plus) CMC, (circle) SLF, (delta) experimental measurement.

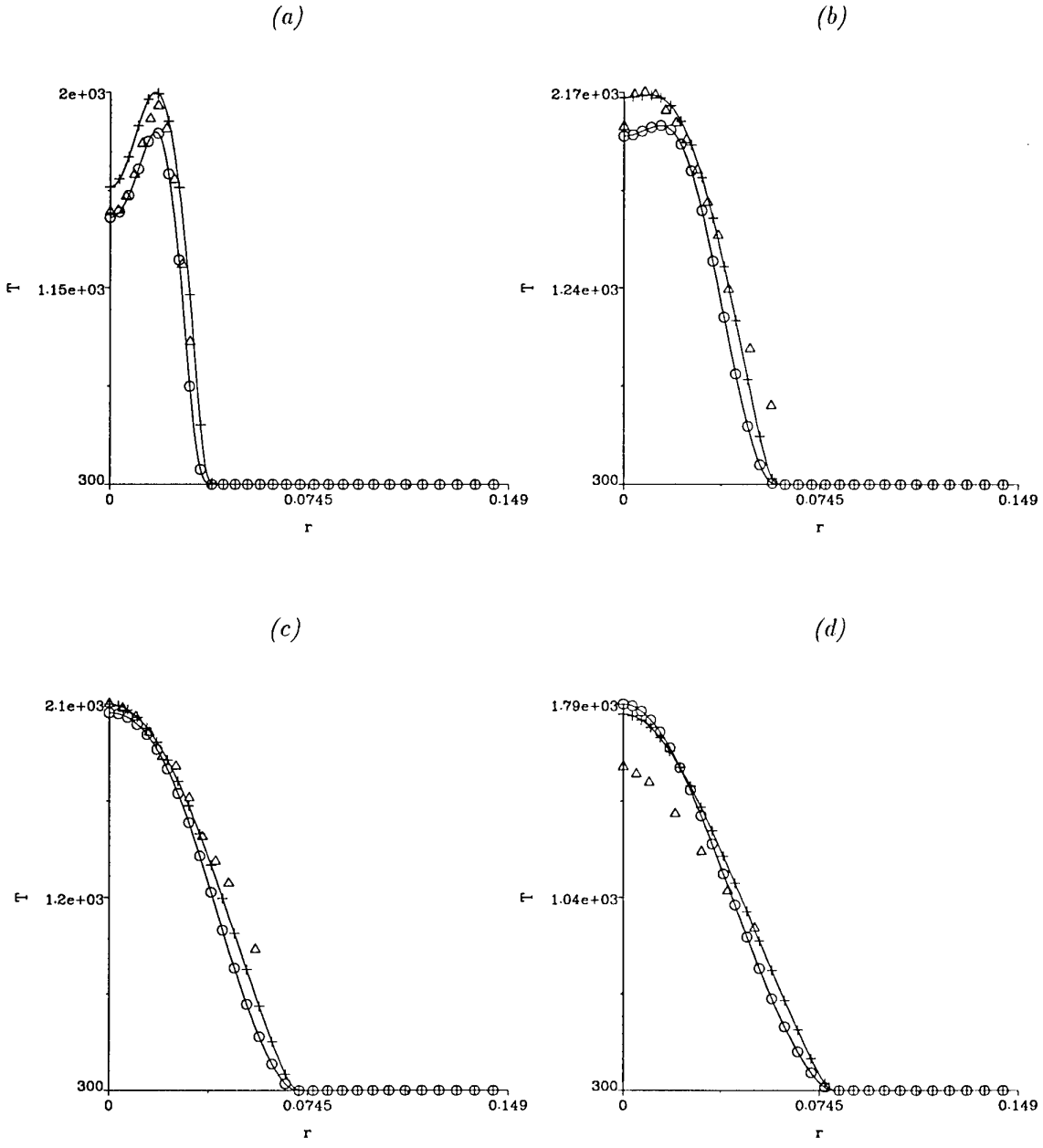

Figure 6: Radial variation in mean temperature at x/D = 45 (a), 90 (b), 135 (c), 180 (d), in flame BC. Note nozzle diameter is 3.75 mm. Symbol key: (plus) CMC, (circle) SLF, (delta) experimental measurement.

4 Discussion

The presence of significant inadequacies in the prediction of the mixture fraction field have tended to cloud the analysis of the thermochemical predictions provided by the CMC and SLF models in the flames studied. While a significant level of agreement between predictions and measurements has been demonstrated, a closer degree of investigation is required if the salient features of the two models are to be uncovered. It is important to determine what these predictive features are in a way that is abstracted from the influence of the peculiarities that may be associated with a predicted mixture fraction field. Future applications of these models in gas turbine combustor (GTC) applications will be far removed from the ordered flow behaviour in a turbulent jet.

Fortunately, in the case of the Barlow and Carter flame at least, extensive experimentally measured conditional mean data is available for comparison with the conditional mean data employed (SLF), and generated (CMC), by the two models.

The comparison of this predicted and measured conditional mean data forms the basis for the discussion on the relevant advantages of the CMC and SLF models, particularly as they apply to more complex combustion systems.

4.1 Conditional mean data comparison

The laser diagnostic techniques employed by Barlow and Carter[3, 39] consist essentially of beaming many laser pulses of extremely short duration through a flame of interest. As the width of each measurement volume is small ($\sim 750\ \mu$m) and the sample duration is short ($\sim 2\ \mu$s), the data collected in this fashion is considered to represent *instantaneous local* thermochemical states, free from temporal and spatial averaging.

In practice, many laser beams of different frequency are directed at the same location in the flame in order to simultaneously measure a wide range of species and temperature. The diagnostic facility described by Barlow and Carter[39] allows the simultaneous measurement of mole fractions of the major species (H_2, O_2, H_2O, N_2), hydroxyl radical (OH), nitric oxide (NO), as well as temperature (through two independent means) at any point in the flame.

Mixture fraction (ξ) is determined from the mass fractions of the species in each sample as the normalised weighted sum of the atomic mass fractions for hydrogen (Z_{hyd}) and oxygen (Z_{oxy}),

$$\xi(\underline{x},t) = \frac{\beta(\underline{x},t) - \beta_{oxidizer}}{\beta_{fuel} - \beta_{oxidizer}}, \tag{15}$$

where the conserved scalar β is defined in terms of atomic mass fractions and atomic weights (W_{oxy},W_{hyd}) by,

$$\beta(\underline{x},t) \equiv \frac{1}{2}\frac{Z_{hyd}}{W_{hyd}} - \frac{Z_{oxy}}{W_{oxy}}. \tag{16}$$

The conserved scalar β has the advantage of being identically zero in a stoichiometric mixture. This gives the resultant mixture fraction the property that its stoichiometric value ($\xi_{stoich} = 0.028$) is fixed independently of whatever differential molecular transport

may be present in the flame. Mixture fraction definitions based upon only one of the participating elemental species, or an inert non-participating species, are subject to changes in the stoichiometric value according to local variations in molecular transport rates.

Laminar flamelet library information for hydrogen-air combustion at one atmosphere pressure with uniform 300 K fuel and air stream temperatures, was generated using the chemical mechanism given in Table 1. The laminar computations were conducted for a one-dimensional opposed flow configuration and allowed for multi-component species transport via the computation of diffusion velocities, but made no allowance for thermal diffusion (only conduction). The derived data was catalogued in terms of the various strain rate cases computed and each data point was ascribed a value of mixture fraction according to the same definition used in the experiments (see Eqn. 15).

Inspection of the computed turbulent mixing field revealed that at the axial locations of $x/D = 45$ & 112, that the stoichiometric contour passed through regions with mean scalar dissipation rates of $\langle\chi\rangle = 1.01$ & $0.06\,s^{-1}$ respectively. These scalar dissipation rates were found to correspond closely with strain rate cases of $a = 126$ & $7.5\,s^{-1}$ by virtue of the approximation,

$$\langle\chi\rangle = 4a\langle\xi\rangle^2(erfc^{-1}([1-\langle\xi\rangle]^2)), \tag{17}$$

provided by Peters[20].

Flamelet data for these strain rate conditions is compared with the appropriate CMC predictions and conditionally averaged experimental data in Figs 7 & 8, which correspond to locations of $x/D = 45$ & 112 in flame BC. In all cases, the curves corresponding to adiabatic chemical equilibrium conditions are also plotted. These equilibrium curves are of course invariant throughout the flame, but serve as a useful reference. In each figure, stoichiometric conditions are present at a mixture fraction of $\eta_{st} = 0.028$, which coincides approximately with the peak values in temperature and radical activity. The reader is reminded that the definition of mixture fraction (Eqn 15) is such that a value of $\eta = 0$ corresponds to a pure oxidizer environment, while $\eta = 1$ corresponds to a pure fuel environment.

4.1.1 Experimentally observed thermochemical behaviour

At the upstream measurement station ($x/D = 45$), it is evident that the flame structure is far removed from chemical equilibrium conditions. The conditional mean temperature profile, measured by experiment, is depressed by as much as 240 K near stoichiometric and at richer ($\eta > \eta_{st}$) mixture fractions. On the lean ($\eta < \eta_{st}$) side of stoichiometric, it appears that the observed temperature profile exceeds chemical equilibrium levels. The observed profile for H_2O mass fraction, the major exothermic product, also deviates from equilibrium conditions, displaying a marked tendency to exceed the equilibrium profile on the rich side. The peak observed level of OH mass fraction is almost double that which corresponds with the equilibrium profile.

At the downstream measurement station ($x/D = 112$), the observed conditional mean temperature profile lies below the equilibrium line at all mixture fractions, but only by at most 110 K. The degree of depression increases with axial distance from the nozzle

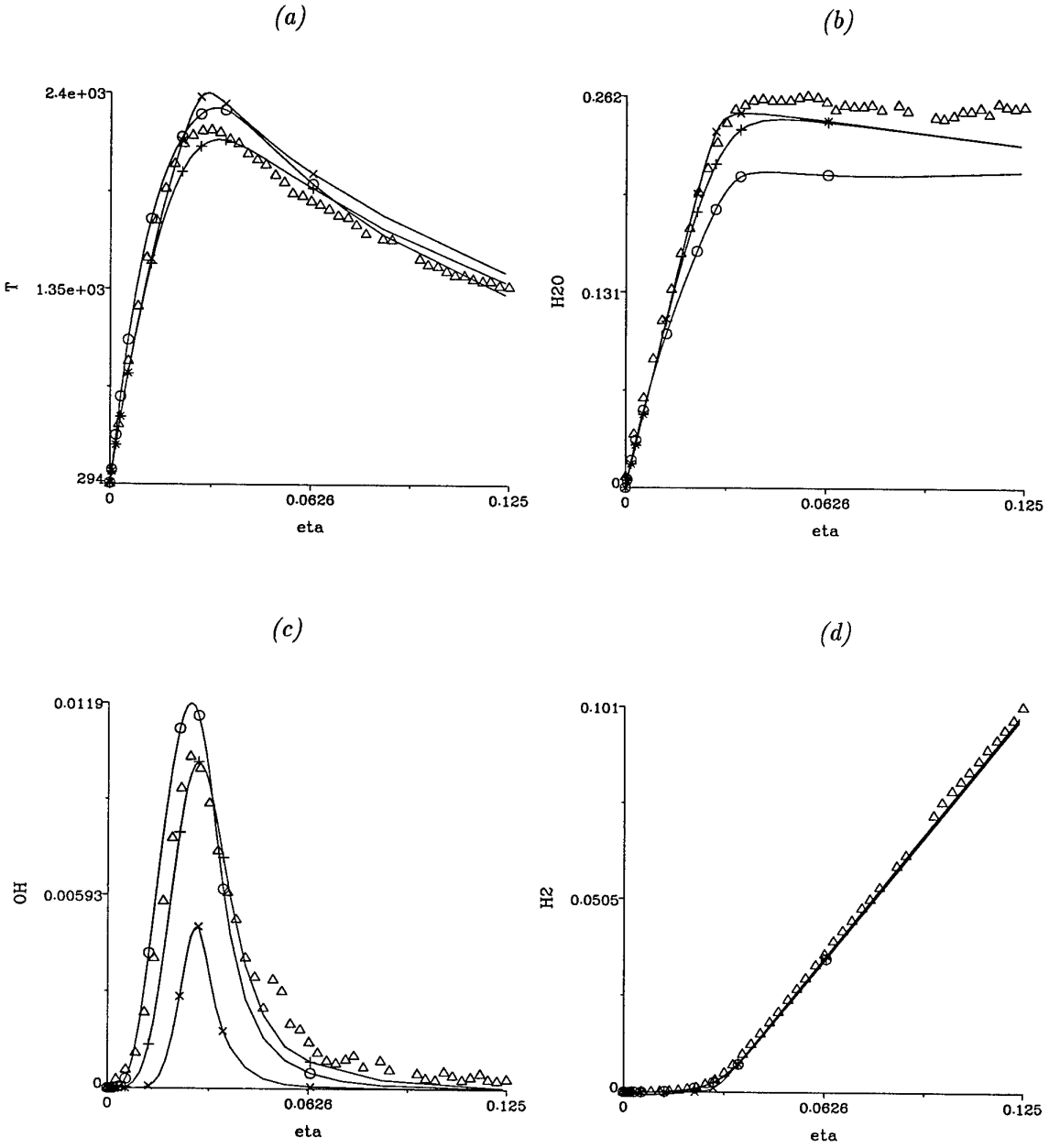

Figure 7: Conditional mean temperature (Kelvins) and species mass fractions data as functions of mixture fraction in flame BC at $x/D = 45$. Symbol key: (cross) fast chemistry, (plus) CMC, (circle) SLF, (delta) experimental measurement.

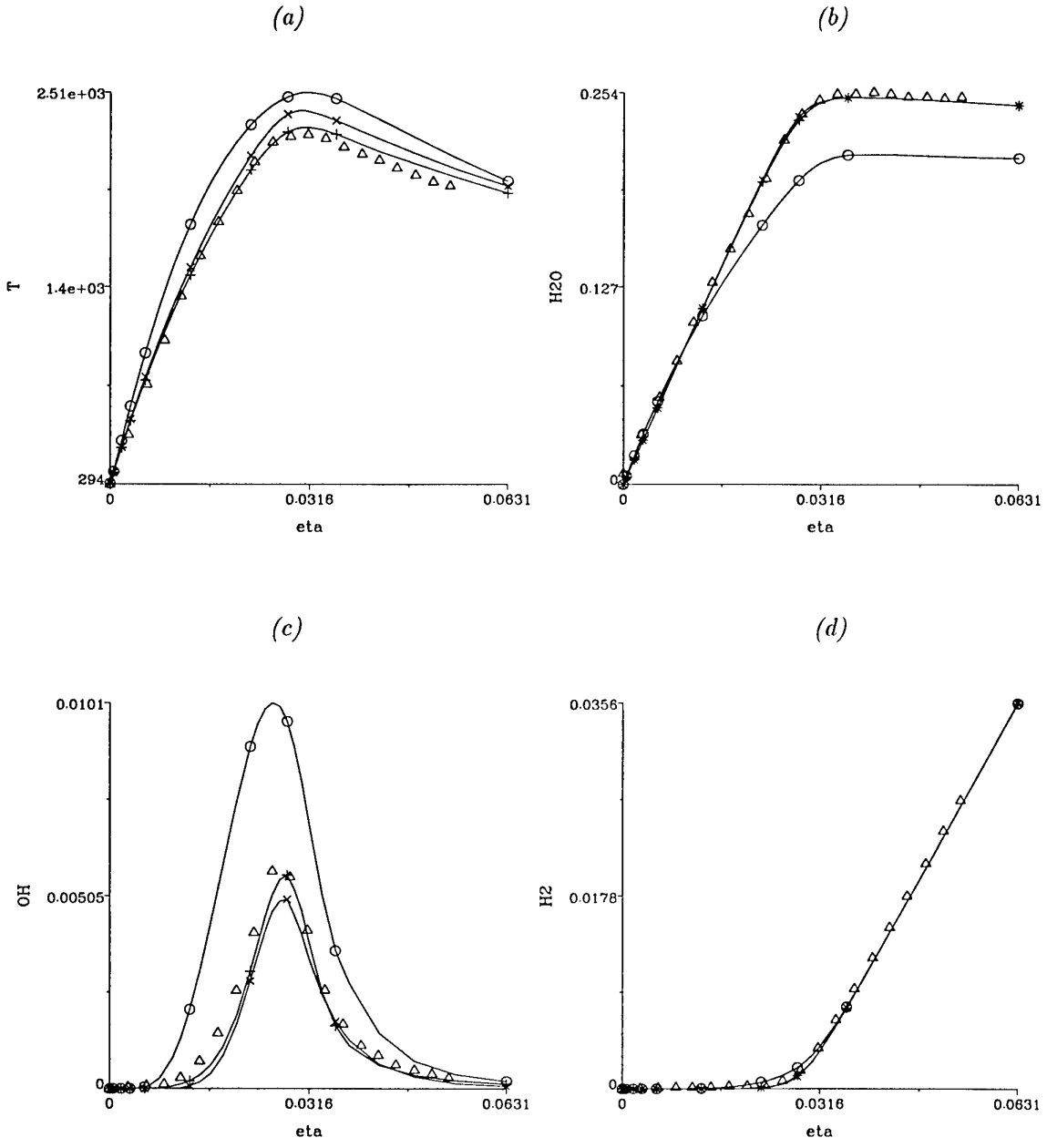

Figure 8: Conditional mean temperature (Kelvins) and species mass fractions data as functions of mixture fraction in flame BC at x/D = 112. Symbol key: (cross) fast chemistry, (plus) CMC, (circle) SLF, (delta) experimental measurement.

(not shown) in accordance with gradual radiant heat loss. The observed conditional mean species mass fraction profiles all lie very much closer to the equilibrium profile at the downstream station than at the upstream station.

This trend in observed thermochemical behaviour is the result of a number of physical processes at work in the jet flame. Firstly, there is the tendency for the level of local mixing intensity to decay rapidly with axial distance from the the nozzle exit plane. Mean scalar dissipation rate, for example, is thought to decay as $\langle\chi\rangle \sim x^{-4}$, although there is some evidence to dispute the high value of the index in the case of jet *flames*[40]. The reduced intensity of mixing with axial length, or equivalently, the lengthened mixing timescale, is less of an obstruction to the natural state-space trajectory of the thermochemical system towards equilibrium.

Close to the nozzle exit plane, where mixing rates are extreme, the corresponding mixing timescales are short enough to be comparable with the timescales of the reactions responsible for the recombination of radical species to form exothermic products (principally reactions 5-10 of Table 1). Turbulent mixing action tends to interrupt the progress to completion of these recombination reactions. The faster reactions responsible for endothermic radical formation (reactions 1f-4b, Table 1), are less affected by this high level of mixing. The result of this differential impact on radical formation and consumption, is to elevate high energy radical levels (such as OH) at the expense of local exothermic yield. Under very strongly mixed conditions, even the faster radical formation reactions can be significantly interfered with, thus leading to instances of local extinction and flame blow-off. Local extinction was not, however, observed in the data of Barlow and Carter.

Away from the more intensely mixed upstream regions of the flame, the reduction in local mixing intensity combined with the gradual recombination of radical species, allows the system to move towards an equilibrium state. Peak radical levels decline, major product yield increases, and temperature recovers upwards towards the equilibrium profile.

It is in the downstream zones, however, that the second determining factor in thermochemical behaviour becomes increasingly apparent. Radiation losses from the flame prevents the system from reaching adiabatic chemical equilibrium. Instead, the progressive drain on sensible enthalpy eventually leads to radical abundance dropping below adiabatic equilibrium levels, and the tendency for temperature to decrease rather than recover upwards to adiabatic equilibrium.

4.1.2 Regimes of heat and mass transfer

A study of the CMC and SLF model predictions in Figs 7 & 8 indicate the different nature of mass and heat transport incorporated into the models themselves. The flamelet model makes use of libraries of flame data gathered from one-dimensional laminar diffusion flames, where species transport at all scales is dominated by molecular diffusion. In contrast, the CMC model computes species transport as though turbulent stirring dominates mass transport at all scales of significance, with the result that species diffusivities are assumed to be uniform.

The effect of differential molecular diffusion is apparent in the SLF predictions for temperature and H_2O at $x/D = 45$. The predicted temperature profile exceeds equilibrium

levels on the lean side of stoichiometric, while the predicted H_2O profile actually peaks at a mixture fraction ($\eta = 0.32$) removed from the principal reaction zone. Qualitative agreement between experiment and the SLF predictions for temperature and H_2O mass fraction is evident.

The nature of the uniform diffusivity CMC predictions is quite different, with the curves for temperature and H_2O being bounded by adiabatic equilibrium values at all mixture fractions. In the absence of differential diffusion, it is not possible for temperature and H_2O yield to exceed equilibrium values at any given mixture fraction. The opposite is true for hydroxyl radical (OH) and hydrogen predictions, where uniform diffusivity predictions are bound to exceed the equilibrium profiles in the absence of significant heat loss.

A comparison of model predictions and experimental data at $x/D = 112$ suggests that the nature of heat and mass transfer is notably different from that observed at $x/D = 45$. The experimental profiles for temperature and H_2O mass fraction are contained within the equilibrium envelope, and are in good agreement with the predictions of the CMC model.

The SLF model predictions, on the other hand, are quite distinct in that the predicted system appears to be close to a completely reacted state. Again, this state is different from an adiabatic equilibrium condition due to the significant species mass transfer between different mixture fractions, that is absent by definition in an equilibrium profile.

As a consequence of these arguments, it appears that at $x/D = 112$, the behaviour of the experimentally observed data is best described by the uniformly diffusive transport which occurs where turbulent stirring dominates the overall mixing process. This is not unexpected since, it has been argued in the past[12] that the bulk of turbulent jet diffusion flames are characterised by small unconditional mean scalar gradients in space but with high levels of turbulent scalar and velocity fluctuations.

Conversely however, it is apparent that nearer to the nozzle, the opposite regime exists where mean scalar gradients are large and turbulent fluctuations are small. In these regions it is evident that the substantial influence of differential molecular transport cannot be neglected.

4.1.3 Effect of transient aerothermochemistry

The influence of differential transport notwithstanding, it is evident from Figs 7 & 8 that the CMC model provides superior quantitative agreement with experimental measurement. This improved level of agreement over that provided by the SLF model can be ascribed to another of the key differences between the two models; namely that the CMC method takes into account aerothermochemical processes with characteristic timescales comparable to the residence time of the flame itself.

Transient influences such as kinetically-limited reactions and radiant losses are not accounted for by the SLF model, which makes use of an ensemble of steady flame data. The most obvious example of this can be seen from a comparison of hydroxyl radical levels between Figs 7 & 8. In the upstream portion of the flame near $x/D = 45$, the SLF, CMC and experimental profiles have peak OH mass fractions of a similar magnitude (~ 0.01) as a result of the immediate effect of the mixing field on the chemical kinetic system (see

section 4.1.1). Further downstream however, the slow reactions responsible for radical consumption have taken their toll on the levels of OH present. The abundance of OH is no longer accurately reflected by the local rate and state of mixing, but will be lower due to prior consumption. This is evident at $x/D = 112$ where the SLF predicted OH profile is only marginally reduced, while the CMC and experimental profiles have been reduced by almost fifty (50) percent.

The presence of many slower reaction pathways in combustion systems of practical interest, highlights the need for a model, such as CMC, which accounts for their effects on flame structure.

4.2 Implications for future work

It is anticipated that both the CMC and SLF models will play a role in future development for the prediction of combustion within gas turbine combustors. At present, the primary goals of development in this context include the incorporation of submodels to account for soot particle formation and destruction, fuel droplet evaporation, and adaptation to allow for complex flow geometries.

The findings of this study make it clear that different regimes of turbulent nonpremixed combustion can exist even in a system as simple as a jet diffusion flame. It was found that the far upstream zones of the flame corresponded closely to flamelet-like combustion, with steep mean scalar gradients and low level turbulent fluctuations. Downstream regions in the flame corresponded to a more distributed mode of combustion where mean gradients were small and turbulent fluctuations large. In gas turbine combustors, it is not clear that a simple locational delineation between zones of flamelet and distributed combustion will be possible, owing to the inherent complexity of the flow.

Bilger[12] provides turbulent and chemical scaling arguments to indicate the bounds of applicability of flamelet combustion. This argument involves a comparison of the magnitude of Kolmogorov-scale scalar fluctuations with the width of the flame reaction zone in reactive scalar space. The scale criterion for flamelet applicability is that the width of the reaction zone in mixture fraction space (ξ_R) must be much less than the characteristic scalar fluctuation at dissipative scales. This can be written in terms of the local root mean square fluctuation of mixture fraction (ξ_{rms}), and turbulent Reynolds number (Re_t) as,

$$\xi_R << C Sc_t^{1/2} \frac{\xi_{rms}}{Re_t^{1/4}}, \tag{18}$$

where C is a constant, argued to be of order unity, and Sc_t is the turbulent Schmidt number.

The criterion expressed in Eqn 18 makes it clear that flamelet combustion will be valid in fully turbulent combustion where turbulence levels are moderate (in terms of Re_t) and yet scalar variations are still large. It should be noted that this scaling relation applies only in the case of a fully turbulent environment, and does not allow for cases where the mean scalar gradient dominates the mean scalar dissipation rate. In instances where the mean gradient is large, it is accepted that a flamelet combustion regime will prevail.

While Bilger has shown that the criterion, as written in Eqn 18, is violated in cold jets, and evidence strongly suggests that it is violated in jet flames, doubts have been raised by others as to the appropriate value of the constant C. Buch *at al.*[41] have cited evidence which suggests that the actual smallest scales of passive scalar variations are at least an order of magnitude greater than Kolmogorov length scales and suggest that C should be set at a value between 11.4 and 25. Thus while the form of the criterion is unchallenged, current uncertainty over the constant of proportionality makes its use problematic in practice.

Of a still more practical concern, is the fact that the evaluation of the criterion requires accurate local information for fluctuations in mixture fraction, turbulent kinetic energy, and the turbulent kinetic energy dissipation rate. The performance of the $k-\epsilon$ turbulence model, in predicting the jet flows studied here, has been less than satisfactory. In gas turbine combustor applications, the flow field is far more complex and involves strong levels of swirl and recirculation. It is known that the $k-\epsilon$ model performs exceptionally poorly under these conditions. This does not bode well for its future use, since it has been seen that poor mixing predictions have a pervasive influence on the accuracy of predicted combustor performance.

The importance of transient aerothermochemical effects (see section 4.1.3) will only increase in combustor predictions compared to the predictions made here. When coupled with soot particle formation, radiant losses become extremely important in determining flame dynamics and heat transfer to surrounding objects. It will not be possible to undertake modelling of gas turbine combustor performance using a pure SLF formulation. It will be necessary to expand the library of steady flamelet information used by the model to include different degrees of radiation-induced enthalpy loss. Soot particle dynamics must also be treated outside the bounds of a flamelet model owing to their non-steady nature.

While the CMC model takes transient effects into account by definition, it becomes very computationally expensive to use when large chemical mechanisms (eg. 30-50 reactive species) must be employed, and/or simplifying geometric assumptions cannot be made. If, for example, it was not possible to make the cross-stream averaged approximation described in Section 2.3.2, then the CMC computations performed in this study would have required two orders of magnitude more computer memory and time to complete. Application of the CMC method to gas combustor flows will have to make careful use of appropriate flow field similarities in conditional statistics in order to avoid an intractable numerical system. The use of appropriate reduced chemical mechanisms is also highly desirable, particularly where those mechanisms have reduced numerical stiffness compared to the original mechanism.

Other issues for the CMC model in a combustor simulation involve the accurate closure of soot formation and destruction rates, given their characteristically high activation temperatures (see section 2.3), and the strong small scale differential diffusion properties of soot particles. A second order chemical closure may be required in this case.

5 Conclusions

It has been found that both the Steady Laminar Flamelet (SLF) and Conditional Moment Closure (CMC) models give reasonable predictions of turbulent nonpremixed flame dynamics when used appropriately.

The comparison of model predictions with experimental data from various sources has shown that the current turbulence model, a $k - \epsilon$ formulation, does not correctly predict the mixing field of jet flames. The $k - \epsilon$ model predicts a rate of decay of centreline mean mixture fraction, and associated radial profiles, that is qualitatively different from that observed.

Despite the error introduced by the turbulence model, examination of conditional mean data from the experiments of Barlow and Carter in comparison with model data suggested the following conclusions.

- There is a distinction in the data between combustion which occurs in a thin laminar flamelet regime, and that which occurs in a distributed reaction regime. The former regime was found within 45 diameters of the nozzle exit plane, while the latter prevailed at the other measurement stations.
- The SLF model provides superior qualitative agreement over the CMC model in the upstream zones where the flamelet-type combustion is evident, but significant quantitative disagreement remains.
- Predictions by the CMC model have been found to closely agree with experimental measurements at all but the flamelet-zone $x/D = 45$ station. The superior agreement yielded by the CMC method is thought to be due to the fact that the model allows for transient aerothermochemical effects throughout the flame such as slow radical recombination and radiation loss.

Ongoing work in the adaptation of these models for use in gas turbine combustor predictions, includes the development of a hybrid SLF-soot-radiation model to account for aerothermochemical flame transients, and a dimensionally simplified zonal CMC model for complex flow geometries. Further, work is being carried out to upgrade the current turbulence model in order to be able to accurately predict realistic combustor flows.

The combined use of the SLF-soot-radiation and CMC models, with the latter acting in a refinement or post-processing role, is expected to yield accurate information about combustor performance that will be useful to both designers and operators of gas turbine engines.

References

1. Kent J. H., Bilger R. W.. 1973. "Turbulent Diffusion Flames". *Fourteenth Symposium (International) on Combustion*, the Combustion Institute. pp615-625.

2. Kent J. H., Bilger R. W.. 1976. "The Prediction of Turbulent Diffusion Flame Fields and Nitric Oxide Formation". *Sixteenth Symposium (International) on Combustion*, the Combustion Institute, Pittsburgh. pp1643-1656.

3. Barlow R. S., Carter C. D.. 1994. "Raman/Rayleigh/LIF Measurements of Nitric Oxide Formation in Turbulent Hydrogen Jet Flames". *Combustion and Flame*, v97, pp261-280.

4. Barlow R. S., Carter C. D.. 1996. "Relationships among Nitric Oxide, Temperature, and Mixture Fraction in Hydrogen Jet Flames". *Combustion and Flame*, v104, pp288-299.

5. Bilger R. W.. 1982. "Molecular Transport Effects in Turbulent Diffusion Flames at Moderate Reynolds Number". *Journal of the American Institue for Aeronautics and Astronautics*, v20, pp962-970.

6. Burke S. P., Schumann T. E. W.. 1928. "Diffusion Flames". *First Symposium on Combustion*, the Combustion Institute, Pittsburgh. pp1-11.

7. Pope S. B.. 1981. "A Monte Carlo Method for the PDF Equations of Turbulent Reactive Flow". *Combustion Science and Technology*, v25, pp159-174.

8. Pope S. B.. 1990. "Computations of Turbulent Combustion: Progress and Challenges". *Twenty-Third Symposium (International) on Combustion*, the Combustion Institute, Pittsburgh, pp591-612.

9. Kerstein A. R.. 1991. "Linear Eddy Modeling of Turbulent Transport. Part 4. Structure of Diffusion Flames". *Combustion Science and Technology*, v81, pp75-96.

10. Kerstein A. R.. 1992. "Linear Eddy Modeling of Turbulent Transport. Part 7. Finite Rate Chemistry and Multi-stream mixing". *Journal of Fluid Mechanics*, v240, p289.

11. Peters N.. 1983. "Local quenching due to flame stretch in nonpremixed turbulent combustion". *Combustion Science and Technology*, v30, pp1-17.

12. Bilger R. W.. 1988. "The Structure of Turbulent Nonpremixed Flames". *Twenty-Second Symposium (International) on Combustion*, the Combustion Institute, Pittsburgh. p475

13. Mell W., Kosaly G., Riley J. J.. 1994. "An Investigation of Closure Models for Nonpremixed Turbulent Reacting Flows". *Physics of Fluids*, v6, pp1331-1356.

14. Stårner S. H., Dibble R. W., Barlow R. S., Fourgette D. C., Long M. B.. 1992. "Joint Planar CH and OH LIF Imaging in Piloted Turbulent Jet Diffusion Flames near Extinction". *Twenty-Fourth Symposium (International) on Combustion*, the Combustion Institute, Pittsburgh, pp341-350.

15. Barlow R. S., Chen J.-Y.. 1992. "On Transient Flamelets and their Relationship to Turbulent Methane-Air Jet Flames". *Twenty-Fourth Symposium (International) on Combustion*, the Combustion Institute. Pittsburgh. pp231-237.

16. Haworth D. C., Drake M. C., Pope S. B., Blint J.. 1988. "The importance of time-dependent flame structures in stretched laminar flamelet models for turbulent jet diffusion flames". *Twenty-Second Symposium (International) on Combustion*, the Combustion Institute, Pittsburgh. p589.

17. Ghoniem A. F., Soteriou M. C., Knio O. M., Cetegen B.. 1992. "Effect of steady and periodic strain on unsteady flamelet combustion". *Twenty-Fourth Symposium (International) on Combustion*, the Combustion Institute, Pittsburgh. p223.

18. Mueller C. J., Driscoll J. F., Sutkus D. J., Roberts W. J., Drake M. C., Smooke M. D.. 1995. "Effect of Unsteady Stretch Rate on OH Chemistry during a Flame-Vortex Interaction: To Assess Flamelet Models". *Combustion and Flame*, v100, pp323-331.

19. Mauss F., Keller D., Peters N.. 1990. "A Lagrangian simulation of flamelet extinction and re-ignition in turbulent jet diffusion flames". *Twenty-Third Symposium (International) on Combustion*, the Combustion Institute, Pittsburgh. p693.

20. Peters N.. 1984. "Laminar diffusion flamelet models in nonpremixed turbulent combustion". *Progress in Energy and Combustion Science*, v10, pp319-339.

21. Peters N.. 1986. "Laminar Flamelet Concepts in Turbulent Combustion". *Twenty-First Symposium (International) on Combustion*, the Combustion Institute, Pittsburgh. pp1231-1250.

22. Klimenko A. Yu.. 1990. "Multicomponent Diffusion of Various Admixtures in Turbulent Flow". *Fluid Dynamics*, v25, pp327-334.

23. Bilger R. W.. 1993. "Conditional Moment Methods for Turbulent Reacting Flow". *Physics of Fluids A*, v5, pp436-444.

24. Smith N. S. A., 1994. *Development of the Conditional Moment Closure Method for Modelling Turbulent Combustion.* PhD Thesis, University of Sydney.

25. Smith N. S. A., 1996. "Conditional Moment Closure of Mixing and Reaction in Turbulent Nonpremixed Combustion", *Annual Research Briefs - 1996*, Center for Turbulence Research. Stanford University / NASA Ames Research Center. pp85-100.

26. Correa S. M., Gulati A.. 1988. "Nonpremixed Turbulent CO/H2 Flames at Local Extinction Conditions". *Twenty-Second Symposium (International) on Combustion*, the Combustion Institute, Pittsburgh. pp599-606.

27. Masri A. R., Dibble R. W.. 1988. "Spontaneous Raman Measurements in Turbulent CO/H2/N2 Flames near Extinction". *Twenty-Second Symposium (International) on Combustion*, the Combustion Institute, Pittsburgh. pp607-618.

28. Starner S.H., Bilger R.W., Dibble R.W., Barlow R.S.. 1990. "Piloted Diffusion Flames of Diluted Methane Near Extinction: Mean Structure from Raman/Rayleigh Fluorescence Measurements". *Combustion Science and Technology*, v70, pp111-133.

29. Barlow R. S., Dibble R. W., Chen J.-Y., Lucht R. P.. 1990. "Effect of Damkohler Number on Superequilibrium OH Concentration in Turbulent Nonpremixed Jet Flames", *Combustion and Flame*, v82, p235

30. Masri A.R., Dibble R.W., Barlow R.S.. 1992. "The Structure of Turbulent Nonpremixed Flames of Methanol Over a Range of Mixing Rates". *Combustion and Flame*, v89, pp167-185.

31. Smith N. S. A.. 1995. "Modeling complex chemical effects in turbulent nonpremixed combustion." *Annual Research Briefs - 1995*, Center for Turbulence Research. Stanford University / NASA Ames Research Center. pp301-322.

32. Kronenburg A., Bilger R. W.. 1997. "Modelling of Differential Diffusion Effects in Nonpremixed Nonreacting Turbulent Flow". *Physics of Fluids*, v9, pp1435-1447.

33. Smith N. S. A., Bilger R. W., Chen J.-Y.. 1992. "Modelling of Nonpremixed Hydrogen Jet Flames using a Conditional Moment Closure Method". *Twenty-Fourth Symposium (International) on Combustion*, The Combustion Institute. pp263-269.

34. Smith N. S. A., Bilger R. W., Carter C. D., Barlow R. S., Chen J.-Y.. 1995. "A Comparison of CMC and PDF Modelling Predictions with Experimental Nitric Oxide LIF/Raman Measurements in a Turbulent H2 Jet Flame". *Combustion Science and Technology*, v105, p357.

35. Klimenko A. Yu.. 1994. "Conditional Moment Closure and Large-Scale Fluctuations of Scalar Dissipation". *Fluid Dynamics*, v28, pp630-637.

36. Launder B. E., Spalding D. B.. 1974. "The Numerical Computation of Turbulent Flows". *Computational Methods in Applied Mechanical Engineering*, v3, pp269-289.

37. Rogg B., Williams F. A.. 1988. "Structure of wet CO Flames with Full and Reduced Kinetic Mechanisms". *Twenty-Second Symposium (International) on Combustion*, the Combustion Institute. pp1441-1451.

38. Miller J. A., Bowman C. T.. 1989. "Mechanism and Modelling of Nitrogen Chemistry in Combustion". *Progress in Energy and Combustion Science*, v15, pp287-338.

39. Carter C. D., Barlow R. S.. 1994. "Simultaneous Measurements of NO, OH and the Major Species in Turbulent Flames". *Optics Letters*, v19, pp299-301.

40. Effelsberg E., Peters N.. 1988. "Scalar Dissipation Rates in Turbulent Jets and Diffusion Flames". *Twenty-Second Symposium (International) on Combustion*, the Combustion Institute, Pittsburgh. pp693-700.

41. Buch K. A., Dahm W. J. A., Dibble R. W., Barlow R. S.. 1992. "Structure of Equilibrium Reaction Rate Fields in Turbulent Jet Diffusion Flames". *Twenty-Fourth Symposium (International) on Combustion*, the Combustion Institute. Pittsburgh. pp295-301.

DISTRIBUTION LIST

Comparison of CMC and SLF model predictions with experimental data for turbulent hydrogen jet flames

Nigel S. A. Smith

	Number of Copies
AUSTRALIAN DEFENCE ORGANISATION	
S&T Program	
Chief Defence Scientist FAS Science Policy AS Science Corporate Management	1
Director General Science Policy Development	1
Counsellor Defence Science, London	Doc Data Sht
Counsellor Defence Science, Washington	Doc Data Sht
Scientific Adviser to MDRC Thailand	Doc Data Sht
Director General Scientific Advisers	1
Navy Scientific Adviser	Doc Data Sht
Scientific Adviser - Army	Doc Data Sht
Air Force Scientific Adviser	1
AMRL Personnel	
Director, Aeronautical and Maritime Research Laboratory	1
Chief, Airframes and Engines Division	1
Research Leader, Propulsion	1
Dr Simon Henbest, AED	1
Author : Nigel S. A. Smith	1
J. Greg Bain	1
DSTO Libraries	
Library, Fishermens Bend	1
Library, Maribyrnong	1
Library, Salisbury	2
Australian Archives	1
Library, MOD, Pyrmont	Doc Data Sht
Capability Development Division	
Director General Maritime Development	Doc Data Sht
Director General Land Development	Doc Data Sht
Director General C3I Development	Doc Data Sht
Army	
ABCA Office, G-1-34, Russell Offices, Canberra	4

SO (Science), DJFHQ(L), MILPO Enoggera	Doc Data Sht
NAPOC QWG Engineer NBCD	Doc Data Sht
Intelligence Program	
DGSTA Defence Intelligence Organisation	1
Corporate Support Program (libraries)	
OIC TRS, Defence Regional Library, Canberra	1
Officer in Charge, Document Exchange Centre (DEC)	1
Copies required by DEC for :	
US Defence Technical Information Center	2
UK Defence Research Information Centre	2
Canada Defence Scientific Information Service	1
NZ Defence Information Centre	1
National Library of Australia	1
UNIVERSITIES AND COLLEGES	
Australian Defence Force Academy	
Library	1
Head of Aerospace and Mechanical Engineering	1
Other Universities	
Deakin University Library, Serials Section (M list)	1
Senior Librarian, Hargrave Library, Monash University	1
Librarian, Flinders University	1
OTHER ORGANISATIONS	
NASA (Canberra)	1
AGPS	1
OVERSEAS	
Abstracting and Information Services	
Engineering Societies Library, US	1
Documents Librarian, The Center for Research Libraries, US	1
Information Exchange Agreement Partners	
Acquisitions Unit, Science Reference and Information Service, UK	1
Library - Exchange Desk, National Institute of Standards and Technology, US	1
SPARES	
Five copies	5

Total number of copies: 45

DEFENCE SCIENCE AND TECHNOLOGY ORGANISATION DOCUMENT CONTROL DATA				1. CAVEAT/PRIVACY MARKING
2. TITLE Comparison of CMC and SLF model predictions with experimental data for turbulent hydrogen jet flames			3. SECURITY CLASSIFICATION Document (U) Title (U) Abstract (U)	
4. AUTHOR(S) Nigel S. A. Smith			5. CORPORATE AUTHOR Aeronautical and Maritime Research Laboratory 506 Lorimer St, Fishermens Bend, Victoria, Australia 3207	
6a. DSTO NUMBER DSTO–TR–0631	6b. AR NUMBER AR-010-468		6c. TYPE OF REPORT Technical Report	7. DOCUMENT DATE March 6th 1998
8. FILE NUMBER MI9439	9. TASK NUMBER DST 95/136	10. SPONSOR DSTO	11. No OF PAGES 30	12. No OF REFS 41
13. DOWNGRADING / DELIMITING INSTRUCTIONS Not Applicable			14. RELEASE AUTHORITY Chief, Airframes and Engines Division	

15. SECONDARY RELEASE STATEMENT OF THIS DOCUMENT

Approved For Public Release

OVERSEAS ENQUIRIES OUTSIDE STATED LIMITATIONS SHOULD BE REFERRED THROUGH DOCUMENT EXCHANGE CENTRE, DIS NETWORK OFFICE, DEPT OF DEFENCE, CAMPBELL PARK OFFICES, CANBERRA, ACT 2600

16. DELIBERATE ANNOUNCEMENT

No Limitations

17. CITATION IN OTHER DOCUMENTS

No Limitations

18. DEFTEST DESCRIPTORS

Diffusion Flames
Turbulent diffusion
Combustion
Gas turbine engines
Combustors

19. ABSTRACT

Jet diffusion flames have long been the basic model problem for developing and verifying models for turbulent nonpremixed combustion. In this report, a comprehensive jet flame study of two well known models is made as a foundation step for the incorporation of these models into DSTO's ongoing effort to develop a fundamentally-based generic gas turbine combustor predictive capability. Conditional Moment Closure (CMC) and Steady Laminar Flamelet (SLF) model predictions are compared with data measured from the two turbulent hydrogen jet flames studied experimentally by Kent and Bilger, and Barlow and Carter. The comparison highlights the advantages and disadvantages of each model in the context of predicting turbulent nonpremixed flame dynamics in general. The future application of these two models to the turbulent nonpremixed systems associated with gas turbine engine combustors is discussed in the light of the findings presented.

VS

[redacted]

TECHNICAL REPORT DSTO-TR-0631 AR-010-468 MARCH 6th 1998

AERONAUTICAL AND MARITIME RESEARCH LABORATORY
PO BOX 4331 MELBOURNE VICTORIA 3001
AUSTRALIA, TELEPHONE (03) 9626 7000